Physical properties of $YbXCu_4$ (X = Ag, Au, Cd, Mg, Tl, and Zn) compounds

J. L. Sarrao,* C. D. Immer, and Z. Fisk
National High Magnetic Field Laboratory, Florida State University, Tallahassee, Florida 32306

C. H. Booth,* E. Figueroa,† and J. M. Lawrence
University of California, Irvine, California 92697

R. Modler, A. L. Cornelius, M. F. Hundley, G. H. Kwei, and J. D. Thompson
Los Alamos National Laboratory, Los Alamos, New Mexico 87545

F. Bridges
University of California, Santa Cruz, California 95064

(Received 16 June 1998; revised manuscript received 16 November 1998)

We report a systematic study of the face-centered-cubic compounds $YbXCu_4$ (X = Ag, Au, Cd, Mg, Tl, and Zn), as well as their corresponding nonmagnetic analogues $LuXCu_4$. X-ray diffraction, heat capacity, magnetic susceptibility, high-field magnetization, electrical resistivity, Hall effect, and L_{III}-edge absorption measurements have been performed. The compounds have Kondo temperatures that range from about 10 K to nearly 1000 K. Although the single-impurity Kondo model qualitatively describes the physical properties of these materials, the quantitative details are not well described and the quality of the fits varies strongly from compound to compound. Compound-to-compound variations in crystal-electric fields, effective valence, and the strength of f-ligand hybridization effects, as well as the influence of intrinsic disorder, may help to explain these discrepancies. [S0163-1829(99)07209-4]

I. INTRODUCTION

Ytterbium compounds display a rich variety of physical properties, in large measure due to Yb's position in the lanthanide row of the periodic table as the ''f-hole'' analogue of Ce, of which many compounds are also known.[1,2] Because of the Hund's rule tendency to fill the $4f$ shell, Yb has two energetically similar electronic configurations, trivalent f^{13} and divalent f^{14}. In many Yb compounds a quantum-mechanical admixture of these states leads to intermediate valence character. The near degeneracy of these configurations implies that small changes in the crystallographic and electronic environment of the Yb ion due to other constituents in a periodic lattice can have large effects on the physical properties of the particular compound being studied.

The physics in these systems derives from hybridization between (nearly) localized f and ligand electrons. In fact, a semiquantitative understanding of the physical properties of Yb compounds has been gained by studying the Anderson-impurity Hamiltonian, which models these correlations for a single f-electron impurity in a metallic host.[3] The Bethe ansatz solution to the Coqblin-Schrieffer model (the Anderson-impurity Hamiltonian in the Kondo limit, where n_f, the f-electron occupation number, is identically unity) describes quantitatively the physical properties of some Yb compounds. It is rather remarkable that these *single-impurity* theories describe the properties of a periodic lattice of magnetic ions as well as they do, and it is well documented that for some compounds the impurity theories do rather poorly.[3] This variation results presumably from competition among several relevant energy scales and interactions in these compounds. In this work, we report a systematic experimental investigation of a set of isostructural Yb compounds to test the applicability of these theories and to deduce the relative strengths of these interactions and, therefore, why some of the data are well-fit quantitatively while in other cases the agreement is qualitative at best.

The compounds investigated are the face-centered-cubic $YbXCu_4$ series, with X = Ag, Au, Cd, In, Mg, Tl, and Zn. The Ag, Au, and In variants are rather well studied and display a broad range of physical properties. $YbAgCu_4$ is a prototypical heavy-Fermion compound that displays a linear specific heat coefficient γ above 200 mJ/mol K^2 with no magnetic order observed to the lowest temperatures measured. It has been claimed that the data for $YbAgCu_4$ can be fit quantitatively to the numerical predictions of the $J=7/2$ Coqblin-Schrieffer model;[4–8] however, the characteristic temperatures that one extracts from fits to various physical properties of $YbAgCu_4$ display a large scatter.[9] In sharp contrast, $YbAuCu_4$ orders magnetically below 1 K, and its low-temperature properties are dominated by long range Ruderman-Kittel-Kasuya-Yosida interactions and crystal-electric-field effects.[4,5,10,11] Finally, $YbInCu_4$ represents the most extreme limit of mixed-valence behavior: a first-order isostructural valence transition is observed at ambient pressure near 40 K, qualitatively similar to what is found in elemental Ce.[12–19] The $YbXCu_4$ compounds for X = Cd and Tl (Ref. 20) are relatively less studied and for X = Mg and Zn are previously unreported; each displays properties intermediate to those discussed above.

In the remainder of the paper we report the data that we have obtained and explore the extent to which the various physical properties, and their variation with X, can be described by single-impurity theories. Experimental details are

 ©1999 The American Physical Society

TABLE I. Lattice constants of YbXCu$_4$ and LuXCu$_4$. With the exception of X=Ag, the amount by which the lattice constant of YbXCu$_4$ exceeds that of LuXCu$_4$ correlates well with $1-n_f(300)$, where the valence of Yb at room temperature, deduced from $L_{\rm III}$ measurements, is $2+n_f(300)$. See text for details.

X	Metallic radius	a_0(YbXCu$_4$)	a_0(LuXCu$_4$)	$\frac{[a_0(\mathrm{Yb})-a_0(\mathrm{Lu})]}{a_0(\mathrm{Lu})}$	$1-n_f(300)$
Ag	1.445 Å	7.083 Å	7.094 Å	−0.155%	0.07
Au	1.442	7.046	7.037	0.128	0.04
In	1.663	7.158	7.148	0.140	0.07
Zn	1.394	7.046	7.034	0.171	0.12
Cd	1.568	7.135	7.123	0.168	0.18
Tl	1.716	7.155	7.125	0.421	0.18
Mg	1.602	7.194	7.129	0.912	0.31

discussed in Sec. II. The structural, specific heat, magnetic, and transport data are reported in Secs. III, IV, V, and VI, respectively. Section VII reports the evolution of the *f*-electron occupation number as a function of temperature, as deduced from $L_{\rm III}$ absorption-edge measurements. In Secs. VIII and IX we attempt to place in context the implications of our results and make suggestions for further study.

II. EXPERIMENTAL DETAILS

When one is attempting to discover intrinsic trends among a range of related compounds, sample quality and characterization are, of course, important in separating potentially extrinsic effects from intrinsic properties. Wherever possible in this study, we have used single crystal specimens and have selected crystals from the same or identically-prepared batches for the wide range of measurements we report. We also have studied the Lu analogues of each of the YbXCu$_4$ compounds in order to separate magnetic and lattice effects. Using a variety of X-Cu fluxes, we have grown single crystals of YbAgCu$_4$, YbCdCu$_4$, YbInCu$_4$, YbTlCu$_4$, and YbZnCu$_4$. Additionally, single crystals of YbMgCu$_4$ were grown from a lead flux. Unfortunately, it has not proved possible to grow single crystals of YbAuCu$_4$, so only data from polycrystalline samples, obtained by slow-cooling stoichiometric ratios of the constituent elements in a sealed Ta tube, are reported. For some measurements, the size of the single crystals of YbMgCu$_4$ and YbZnCu$_4$ were inadequate, and polycrystalline samples, prepared identically to the YbAuCu$_4$ material, were studied after verifying that the lattice constant, magnetic susceptibility and electrical resistivity were identical to the smaller single crystals. For each of the above-listed YbXCu$_4$ compounds, the LuXCu$_4$ variants were prepared similarly.

A wide range of experimental techniques has been employed to fully characterize the physical properties of these materials. Lattice constants were determined with high-resolution powder x-ray diffraction using internal silicon reference material to correct for systematic errors. A thermal relaxation technique was used to determine specific heat for $1.5\,\mathrm{K}\leqslant T\leqslant 20\,\mathrm{K}$. A superconducting-quantum-interference-device magnetometer was used to measure the temperature-dependent magnetic susceptibility and to provide an absolute calibration to high-field magnetization measurements. The high-field magnetization measurements were performed using a mutual inductance technique in a 600 kOe pulsed magnet located at the National High Magnetic Field Laboratory–Los Alamos Pulsed Field Facility. Electrical resistivity measurements as a function of temperature were performed in the standard four-wire configuration, and Hall voltage was measured in fields of ±10 kOe using an LR400 ac resistance bridge. X-ray absorption data were collected at the Stanford Synchrotron Radiation Laboratory on beam line 2-3. Data were collected for the YbXCu$_4$ samples from below the Yb $L_{\rm III}$ edge (8944 eV) to above the Cu K edge (8979 eV). Data also were collected for the Lu $L_{\rm III}$ edge (9244 eV) on the counterpart f^{14} LuXCu$_4$ samples. A copper foil was used as an energy reference for all samples, and a ''pre-edge'' subtraction was performed on the data using a Victoreen formula to remove the contribution of other absorption processes.

III. LATTICE PARAMETERS AND STRUCTURAL PROPERTIES

The RXCu$_4$ compounds (R=Yb or Lu; X=Ag, Au, Cd, In, Mg, Tl, Zn) crystallize in the cubic AuBe$_5$ (C15b) crystal structure. In the ideal structure, the R and X ions sit on distinct face-centered-cubic lattices displaced by (1/4, 1/4, 1/4) along the body diagonal and are surrounded by space-filling Cu tetrahedra centered at (x,x,x), with $x\approx 3/4$. The disordered Laves phase MgCu$_2$ (C15) variant of this structure has random occupation of the (0, 0, 0) and (1/4, 1/4, 1/4) sublattices by R and X. By x-ray diffraction these structures can be distinguished because the reflections that satisfy the selection rule $h+k+l\neq 4n$, where n is an integer and h, k, and l are even, are allowed only in the ordered structure.[21] For each of the compounds we have studied, we observe the (200), (222), and (622) reflections, indicating that the R and X sublattices are ordered. As will be discussed below, we cannot rule out some X-Cu site disorder, except based on empirical ionic size arguments. We observe no evidence for second phases in either our single crystal or polycrystalline samples.

The measured values of the lattice constants for RXCu$_4$ at room temperature are shown in Table I. For the Lu compounds, the lattice constants appear to be governed by the metallic radii of the X elements, as would be expected due to space-filling considerations. The LuXCu$_4$ lattice constants a_0 increase in the order X=Zn, Au, Ag, Cd, Tl, Mg, In, while the metallic radii increase in the order X=Zn, Au, Ag, Cd,

Mg, In, Tl, so that only the lattice constant of LuTlCu$_4$ is anomalous. Except for YbAgCu$_4$, discussed below, the YbXCu$_4$ lattice constants are consistently larger than their LuXCu$_4$ counterparts at room temperature. This is due to the mixed-valent nature of Yb. Trivalent Yb and trivalent Lu are nearly identical in size, whereas divalent Yb is significantly larger. Thus, the amount by which the YbXCu$_4$ lattice constant exceeds that of LuXCu$_4$ is an approximate measure of the degree of mixed valence for that compound.

The case of X=Ag is anomalous. It is the only compound for which the lattice constant of YbXCu$_4$ is smaller than that of LuXCu$_4$, a result which is hard to understand based on the size arguments discussed above. As observed in the thermal expansion data of Cornelius *et al.*,[14] this difference persists to low temperature. Despite the fact that the temperature dependence of $a_0(\mathrm{YbAgCu_4})-a_0(\mathrm{LuAgCu_4})$ is essentially identical to the measured $1-n_f(T)$ for YbAgCu$_4$, the lattice constant of YbAgCu$_4$ remains smaller than that of LuAgCu$_4$ as a function of decreasing temperature.[14] Although we have no explanation for this observation, we speculate that $4d/5s-4f$ hybridization, which can be very strong, may tend to collapse YbAgCu$_4$ relative to LuAgCu$_4$. Mg, Cd, and Zn are closed-shell elements, and Tl and In have one p electron. Both Ag and Au are in $d^{10}s^1$ configurations, but Au has 32 more electrons than Ag, so hybridization effects may be weaker there. Counter to this hypothesis is the fact that the lattice constant of the recently-reported face-centered-cubic phase of YbCu$_5$ (Ref. 22) is comparable to that of LuCu$_5$,[23] a case where hybridization effects should be even more pronounced.

IV. SPECIFIC HEAT

One of the characteristic features of mixed-valent materials is an enhanced electronic contribution to the low-temperature specific heat C_p. We have measured the specific heat for each of our YbXCu$_4$ compounds, as well as for LuXCu$_4$ in order to correct for the nonmagnetic contribution. The data were plotted as C_p/T versus T^2, from which the linear electronic coefficient γ and the cubic phonon contribution β could be easily extracted. Fits were performed below 5 K when reasonable so that the lattice term β remained cubic with T, i.e., the Debye approximation remained valid. In some cases, fitting the data over this temperature range was not reasonable (see the YbZnCu$_4$ fit in Fig. 1), so data at higher temperature were fit. The results of these fits are reported in Table II. The upturn in C_p/T at low temperature for YbZnCu$_4$ might suggest magnetic ordering; however, no bulk ordering is observed above $T=100$ mK. Further measurements are in progress to more fully characterize the low-temperature properties of YbZnCu$_4$. Figure 1 shows data for YbCdCu$_4$ and YbZnCu$_4$, the two YbXCu$_4$ compounds with the largest, previously unreported linear coefficients of specific heat.

All of the specific heat data were reasonably fit by $C_p/T=\gamma+\beta T^2$ except for that of YbAuCu$_4$.[4] These data were best fit by including a Schottky contribution to account for crystal-field splitting (Fig. 2), as previously observed by inelastic neutron scattering.[5] Analysis of the neutron data suggests that the ground state is a doublet and the first excited state is a quartet.[5] We could not obtain high quality fits

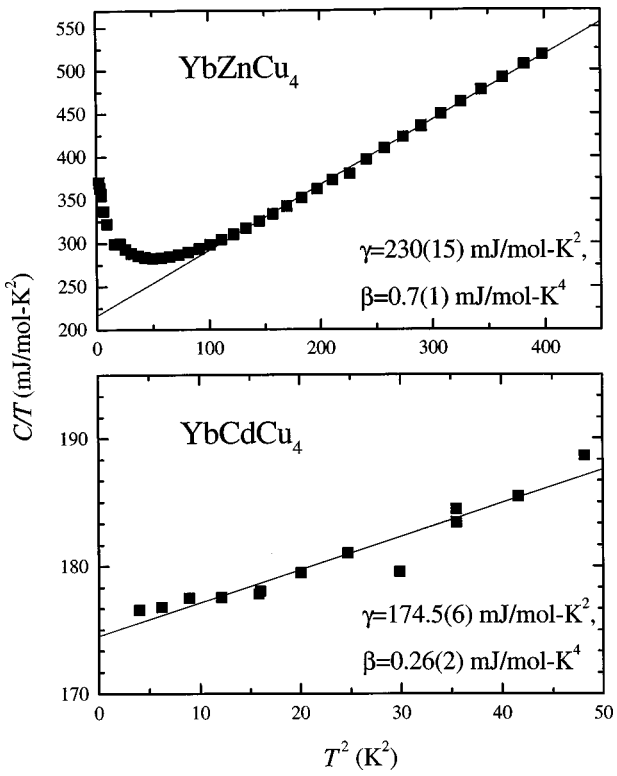

FIG. 1. Specific heat divided by temperature versus temperature squared for YbZnCu$_4$ and YbCdCu$_4$.

to our specific heat data with this crystal-field arrangement. The data were best-fit with a doublet ground state and a doublet first excited state about 3 meV above the ground state. The energy of the second excited level, which then must be a quartet, is more difficult to determine from our low-temperature data but is at least 7 meV above the ground state. Although the relative degeneracies of the crystal-field levels deduced from our Schottky analysis differ from the neutron analysis, the energy spacing of the excited states deduced from the two experiments is consistent.

V. MAGNETIC PROPERTIES

Magnetic susceptibility data for each of the YbXCu$_4$ compounds are shown in Fig. 3. These data bear some similarities to the predictions of the Coqblin-Schrieffer model[24] and to calculations based on the Anderson Hamiltonian in the noncrossing approximation (NCA).[25] Namely, deviations from Curie-Weiss behavior are observed in each case, and shoulders or local maxima at low temperature are common. However, the relative size of the maximum in $\chi(T)[\chi_{\max}/\chi(0)]$ is not a universal constant for these materials, counter to the prediction of the Coqblin-Schrieffer model for fixed angular momentum J. For instance, YbAgCu$_4$ and YbTlCu$_4$ show a pronounced maximum in the susceptibility, while YbAuCu$_4$ and YbZnCu$_4$ do not show any evidence of a maximum. The other materials have intermediate values of $\chi_{\max}/\chi(0)$. Estimates of $\chi(0)$, after accounting for extrinsic Curie tails that correspond to less than 1% $J=7/2$ impurity and using a Coqblin-Schrieffer form for the intrinsic contribution to $\chi(T)$ (Ref. 24) (discussed below), are reported in Table II for each of the YbXCu$_4$ com-

TABLE II. Electronic specific heat coefficients and Debye temperatures inferred from specific heat measurements for YbXCu$_4$ and LuXCu$_4$, and $\chi(0)$ inferred from fitting the $\chi(T)$ data of Fig. 3 to the Bethe ansatz, after accounting for a small impurity tail, for the YbXCu$_4$ compounds, and an estimate of $\chi(0)$ for their lutetium analogues. For the Yb compounds the Wilson ratio inferred from $\chi(0)$ and γ_{Yb}-γ_{Lu} is also given.

	Yb				Lu		
X	γ (mJ/mol K^2)	Θ_D (K)	$\chi(0)$ (emu/mol)	$\mathcal{R}$	γ (mJ/mol K^2)	Θ_D (K)	$\chi(0)$ (emu/mol)
Au	150(60)	235(15)			9.7(5)	265(1)	
Zn	230(15)	254(12)	0.034(3)	1.6(2)	7.2(5)	290(1)	$1.0(2)\times10^{-4}$
Cd	175(6)	353(9)	0.015(3)	1.0(2)	9.4(5)	266(1)	$1.9(2)\times10^{-4}$
Ag	209(1)	279(9)	0.0165(1)	0.88(1)	10.1(1)	257(1)	$-1.5(2)\times10^{-4}$
Mg	62(1)	353(14)	0.00397(5)	0.76(2)	8.7(5)	290(2)	$1.3(2)\times10^{-4}$
Tl	31(6)	240(4)	0.0042(1)	1.99(8)	6.8(5)	260(1)	$2.9(2)\times10^{-6}$

pounds (with the exception of $X=$Au, which orders magnetically at low temperature) and their lutetium analogues (data not shown). As can be seen, there is a significant enhancement of $\chi(0)$ for each YbXCu$_4$ as compared to its Lu counterpart, consistent with their enhanced linear coefficient of specific heat. Table II also reports the Wilson ratio $\mathcal{R}=(\pi^2R/3C)\chi(0)/\gamma$ for each compound, where R is the gas constant and C is the Curie constant for $J=7/2$ Yb for each compound.

Within the Bethe ansatz solution of the Coqblin-Schrieffer model,[24] the zero-temperature susceptibility is related to the Kondo temperature T_0 very simply[24]

$$T_0=\frac{\nu(\nu^2-1)(g\mu_B)^2}{24\pi k_B\chi(0)}, \tag{1}$$

where ν is the magnetic degeneracy, g is the Landé g factor, μ_B is the Bohr magneton, and k_B is Boltzmann's constant. For $J=7/2$ and $g=8/7$, appropriate for the full Yb multiplet, $T_0\ \chi(0)=3.28$ with T_0 in K and $\chi(0)$ in emu/mol. The simplest estimate of T_0 for the YbXCu$_4$ materials can be made by assuming $J=7/2$ and calculating T_0 from the deduced $\chi(0)$ in Table II. These values, reported as $T_0(\chi_0)$, are shown in Table III.

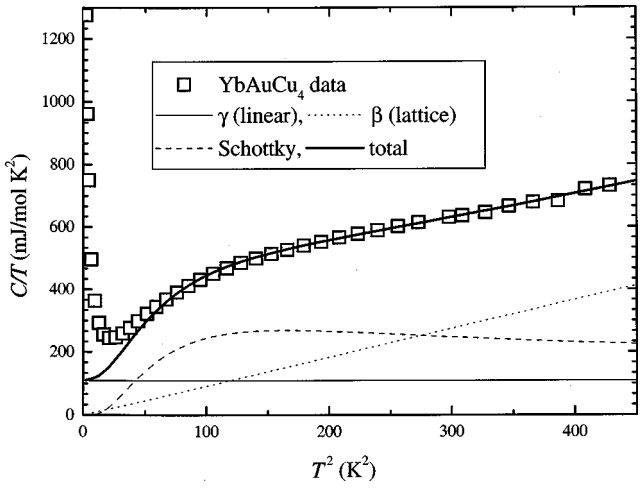

FIG. 2. Specific heat data for YbAuCu$_4$. The open squares are data and the thick solid line is the fit, which consists of electronic, lattice, and Schottky contributions. See text for details.

The temperature dependence of the magnetic susceptibility can be calculated numerically using the Bethe ansatz solution of the Coqblin-Schrieffer model.[24] Fits to the data using this approximation are shown as the solid lines in Fig. 3. (Because YbAuCu$_4$ orders magnetically at low temperature, a ground state clearly inconsistent with a single-impurity interpretation, we do not attempt to fit these data.) The data are not well fit by assuming $J=7/2$ for each of the YbXCu$_4$ compounds. In order to parametrize the variation in $\chi_{\max}/\chi(0)$ that we observe, we fit the data using curves for various J from the calculations of Rajan.[24] In these fits, we find that with the exception of YbAgCu$_4$, the J that produces the best fit increases as T_0 increases ($J=1/2$, 7/2, 3/2, 5/2, 7/2 for $X=$Zn, Ag, Cd, Mg, Tl, respectively, in order of increasing T_0); even for YbAgCu$_4$, although the model captures the qualitative details of the temperature dependence of the susceptibility, quantitatively the fit is less than excellent. Possible mechanisms for variations in $\chi_{\max}/\chi(0)$, including those that might give rise to reduced J, will be discussed in Sec. VIII. T_0's inferred from fitting the temperature-dependent data (using reduced J, where appropriate) are also reported in Table III as $T_0(\chi_{\mathrm{fit}})$.

In Fig. 4, we show the isothermal magnetization for YbXCu$_4$ measured at 4 K for fields up to 500 kOe. Only the data for YbAuCu$_4$ approach the expected free-ion value of the saturated moment ($gJ=4\mu_B$). For the other YbXCu$_4$'s there appears to be a rough scaling of the data with Kondo temperature. The magnetization at 500 kOe decreases with increasing T_0. However, only YbAgCu$_4$ shows the expected upward curvature for a $J=7/2$ magnetic impurity as calculated by Hewson and Rasul.[26] (It should be pointed out that even for $H=500$ kOe, H/T_0 is sufficiently small for YbMgCu$_4$ and YbTlCu$_4$ that upward curvature in the magnetization would not be expected.) Calculations for different J (Ref. 26) reveal that the amount of expected curvature decreases with decreasing J. Therefore, although we have not explicitly fit the magnetization data, it is reasonable to expect that similar values of ''best-fit'' J would be inferred as from the susceptibility fits. Because M vs H is essentially linear over a wide field range for most of the YbXCu$_4$ compounds,

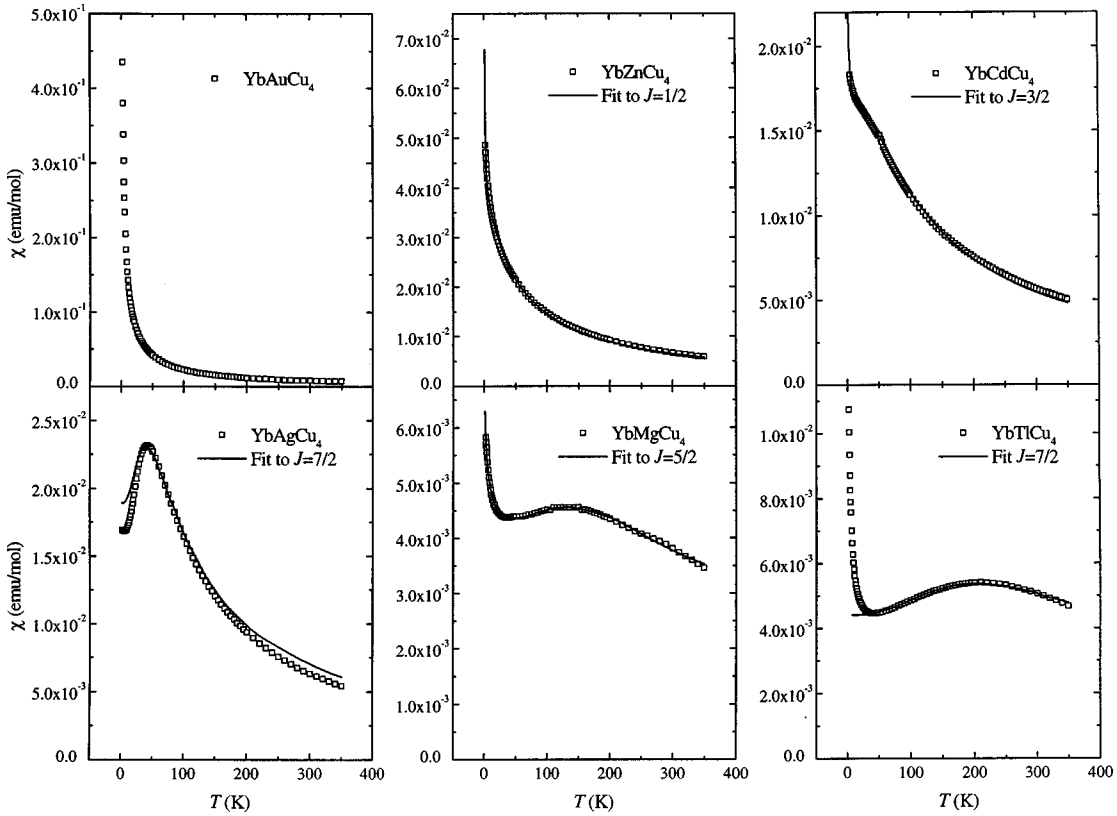

FIG. 3. Susceptibility $\chi(T)$ as a function of temperature for YbXCu$_4$ (X=Au, Zn, Ag, Cd, Mg, and Tl). $\chi(T)$ at low temperatures for all X except Ag is influenced by a small impurity tail. All features of the intrinsic data can be fit to the single impurity model except the relative size of the maximum in $\chi(T)$.

a separate estimate of $\chi(0)$ can be made from the slope of these lines. With the exception of YbTlCu$_4$, for which the M vs H slope implies a value of $\chi(0)$ nearly double that reported in Table II (because of its high T_0 YbTlCu$_4$ is particularly sensitive to sample to sample variations in low-temperature susceptibility), the magnetization slopes are in good agreement with the data of Fig. 3.

VI. TRANSPORT PROPERTIES

The electrical resistivity for each of the YbXCu$_4$ compounds is shown in Fig. 5. Both YbAuCu$_4$ (Ref. 10) and YbAgCu$_4$ (Refs. 7 and 8) have been studied extensively. They each show appreciable drops in resistivity at low temperature; however, studies of resistivity as a function of pressure show that these effects are of different origin. For YbAuCu$_4$ the low-temperature downturn is insensitive to pressure and can be attributed to the depopulation of crystal field levels[5,10] (recall also the specific heat data of Sec. IV and Fig. 2). The position of the maximum in resistivity for YbAgCu$_4$ is strongly pressure dependent, and the drop in resistivity is due to the onset of coherence.[7,8] For X=Cd, Mg, and Tl, similar features in resistivity are observed that, given our estimates of T_0, may be attributable to coherence effects. Measurements of resistivity under pressure for these compounds would be useful in confirming this supposition. Finally, the resistivity of YbZnCu$_4$ shows an upturn at low temperature that one might naively attribute to lattice disorder effects; however, the upturn can be completely suppressed with a 300 kOe magnetic field (see inset Fig. 5). The small upturn in resistivity observed at low temperature in YbCdCu$_4$ can also be suppressed in a magnetic field. The data are reminiscent of CeNiSn and CePd$_3$ and perhaps suggest that YbZnCu$_4$ is a ''failed Kondo semimetal.'' [27]

TABLE III. T_0 estimated from the zero-temperature susceptibility $T_0(\chi_0)$ and from full fits to the Bethe ansatz $T_0(\chi_{\rm fit})$.

X	$T_0(\chi_0)$	$T_0(\chi_{\rm fit})$
Zn	97(10)	31(3)
Cd	221(45)	101(5)
Ag	199(5)	181(15)
Mg	855(10)	525(20)
Tl	740(15)	900(20)

The Hall coefficients R_H of the YbXCu$_4$ and LuXCu$_4$ compounds (X=Au, Zn, Cd, Mg, Tl) in the range 15–325 K are shown in Fig. 6 (see also Ref. 28). Results for X=Ag and In which were reported previously[14] are not shown here. Our results for YbAuCu$_4$ are in agreement with those reported by other authors.[29] For the LuXCu$_4$ compounds with X=Au, Zn, Cd, Mg, R_H is small ($-[0.3-1.7]\times10^{-10}$ m^3/C), negative, and weakly temperature dependent. For LuTlCu$_4$, R_H is even smaller in magnitude but positive below 25 K; this may represent extrinsic behavior. Small Hall coefficients suggest that these are good metals. In a simple one-band model for these compounds, a Hall coefficient of -1×10^{-10} m^3/C corresponds to 5.6 electrons per formula unit. We have discussed previously[28] the connection between the fact that for LuXCu$_4$ a large Hall coefficient (and hence semimetallic be-

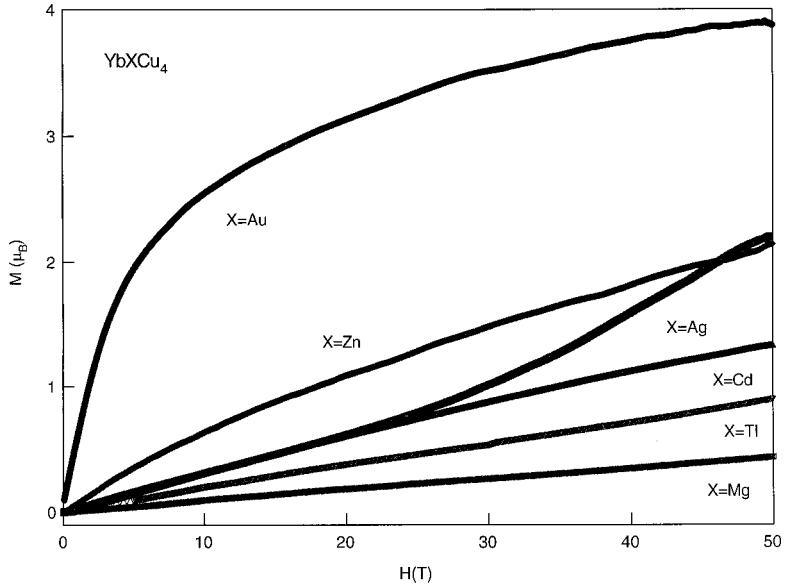

FIG. 4. Isothermal magnetization of YbXCu$_4$ at 4 K, measured using a 600-kOe pulsed magnet.

havior) occurs only in LuInCu$_4$ (Ref. 14) and the fact that for YbXCu$_4$, only YbInCu$_4$ exhibits an isostructural valence transition. Here we focus on the temperature dependence of R_H for the other Yb compounds.

The Hall coefficients of YbXCu$_4$ for $X=$Au, Cd, Tl, Mg are also small, being in the range $-(1-10)\times10^{-9}$ m^3/C. For YbZnCu$_4$ the Hall coefficient reaches the value -20×10^{-9} m^3/C at the lowest temperature measured, consistent with the low-temperature upturn in resistivity. Comparison to the LuXCu$_4$ compounds suggests that the temperature dependence of R_H observed in YbXCu$_4$ is not due to changes in the carrier density, but rather is associated with scattering from the Yb $4f$ electrons. We therefore fit the data to the formula:

$$R_H(T)=R_0(T)+\eta(g\mu_B/k_B)[\chi(T)/C]\rho_{\mathrm{mag}}(T). \quad (2)$$

The first term $R_0(T)$ is the ordinary Hall effect, which we assume to be equal to $R_0+R_H(T;\mathrm{Lu})$, where R_0 is a constant and $R_H(T;\mathrm{Lu})$ is the temperature-dependent Hall coefficient of the corresponding LuXCu$_4$ compound. The second term represents skew scattering of the conduction electrons from Kondo impurities.[30] For this term we again use $g=8/7$, the Landé g factor for a free Yb ion, and we scale the measured susceptibility $\chi(T)$ by C, the $J=7/2$ Yb Curie constant. The quantity $\rho_{\mathrm{mag}}(T)$ is the magnetic resistivity due to scattering from the $4f$ electrons with the normal (e.g., phonon) contributions subtracted. For all X except $X=$Tl we have fit the data assuming $\rho_{\mathrm{mag}}(T)=\rho(T)-\rho(T;\mathrm{Lu})$, i.e.,

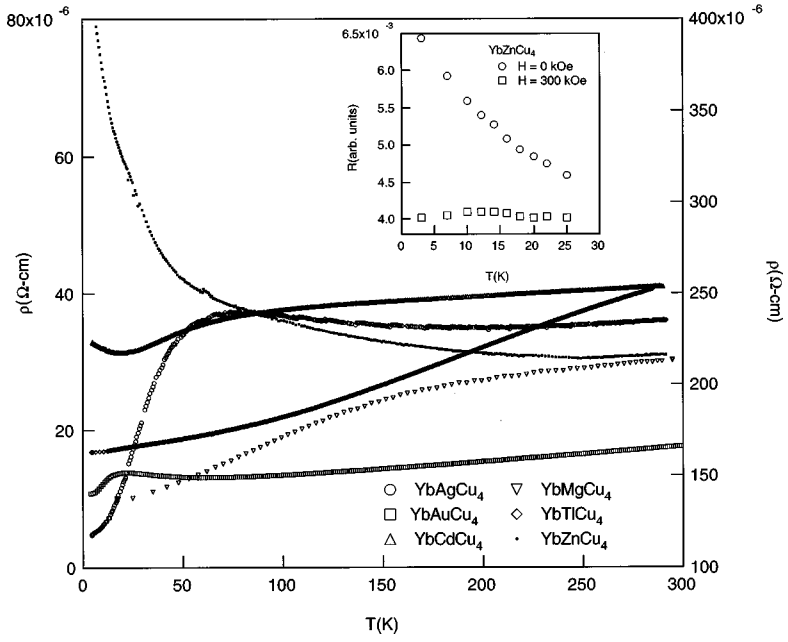

FIG. 5. Electrical resistivity as a function of temperature for YbXCu$_4$. All data are plotted on the left axis except for YbZnCu$_4$, which uses the right axis and includes a zero offset. The inset shows the magnetic field dependence of YbZnCu$_4$'s resistivity.

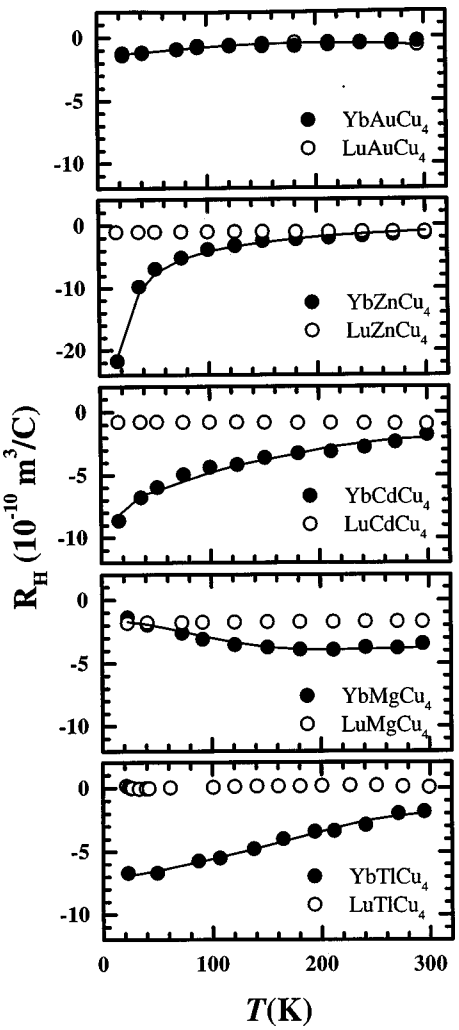

FIG. 6. The Hall coefficient vs temperature for YbXCu$_4$ (closed circles) and LuXCu$_4$ (open circles). The solid lines represent fits to Eq. (2); the values of the fit parameters R_0 (in units of 10^{-10} m^3/C) and η (dimensionless) for the different X are as follows. Au: -0.037, 0.007; Zn: 2.2, -0.074; Cd: 1.0, -0.163; Mg: 1.3, -1.22; Tl: -7.9, 0.97.

subtracting the resistivity of the corresponding LuXCu$_4$ compound as an estimate of the phonon contribution. Because the measured resistivity of LuTlCu$_4$ is larger than that of YbTlCu$_4$, for this case we have equated $\rho_{\rm mag}(T)$ to the measured resistivity data for YbTlCu$_4$ without subtraction of a phonon term. The fits to Eq. (2) are shown in Fig. 6; the values for R_0 and η are given in the caption. For X=Au, Zn, Cd, and Mg the quantity R_0 is small so that the total ordinary Hall coefficient $R_0(T)=R_0+R_H(T;\mathrm{Lu})$ remains small, in the range $(-2\rightarrow+2)\times10^{-10}$ m^3/C. For YbTlCu$_4$, R_0 is somewhat larger, giving a total value of $R_0(T)$ of order -8×10^{-10} m^3/C, which corresponds to a carrier density of 0.7 electrons per formula unit. Hence, the YbXCu$_4$ compounds with X=Au, Zn, Cd, and Mg are reasonable metals, while YbTlCu$_4$ appears to border on semimetallic behavior.

The dimensionless factor η is seen to be vanishingly small for YbAuCu$_4$, negative for X=Zn, Co, and Mg, and positive for X=Tl [and also for X=Ag (Ref. 14)]; a negative η is typical of Yb compounds.[31] In theory[30] η should approximately equal sin δ_2 where δ_2 is the phase shift for nonresonant scattering (e.g., potential scattering in the d channel). This phase shift should not be large, indeed values as large as 0.2 are deemed unrealistic.[30] For the more strongly mixed valent compounds YbTlCu$_4$ and YbMgCu$_4$, values of the parameter η given in Fig. 6 are an order of magnitude larger than the value ($\leq$0.1) expected based on the skew-scattering model.[30] For X=Au, where the ground state multiplet is certainly split by crystal fields, and perhaps for Zn, for which $J=1/2$ is also suggested by our magnetic susceptibility data, the parameters $C_{7/2}$ and $g=8/7$ in Eq. (2) should be replaced by smaller values of $C_{\rm eff}$ and $g_{\rm eff}$ appropriate to the reduced multiplicity of the Yb ground state. This replacement would reduce the fitted values of η considerably. YbCdCu$_4$ is again an intermediate case, with $\eta=0.16$ being somewhat larger than expected based on the model. A possible reason for the large discrepancies for the large T_0 compounds (X=Tl and Mg) is that the skew-scattering theory[30] is only applicable to the high temperature ($T>T_0$) state, whereas these compounds are in the coherent state ($T<T_0$) for the temperatures studied. This is consistent with the fact that an appropriately small value $\eta=+0.07$ was found in YbAgCu$_4$ for $T>T_0$.[14]

VII. $L_{\rm III}$ X-RAY ABSORPTION

In order to directly estimate the temperature dependence of the f-electron occupation number, $n_f(T)$, we have measured the Yb $L_{\rm III}$ absorption edge as a function of temperature for each of the YbXCu$_4$ compounds. For intermediate valence compounds, the Yb edge $\mu_{\rm tot}(E)$ is made up of a divalent $\mu_{2+}(E)$ and a trivalent part $\mu_{3+}(E)$:

$$\mu_{\rm tot}(E)=(1-n_f)\mu_{2+}(E)+n_f\mu_{3+}(E). \qquad (3)$$

The divalent absorption edge is $\sim$7.2 eV lower than the trivalent edge in these metallic systems. In order to fit the data, one would like a purely divalent and a purely trivalent example of the Yb $L_{\rm III}$ edge in a related material. As no such material was available, we used the Lu $L_{\rm III}$ edge from the related LuXCu$_4$ systems. The electronic structure of Lu^{3+} is roughly the same as Yb^{2+}(f^{14}), and should therefore give a good measure of the shape and magnitude of the Yb^{2+} edge. Because the height of the edge is proportional to the number of states available at and above the Fermi level and because these states have s and d symmetry for an excited $2p_{3/2}$ electron, the shape of the Yb^{3+} edge should be almost identical to the Yb^{2+} edge. The isostructural LuXCu$_4$ analogues are also useful because contributions to the edge height from the extended x-ray-absorption fine structure (EXAFS) (especially from multiple scattering effects in the white line) are at least partially accounted for in the analysis. We therefore determine the mean valence of the Yb ions by fitting the Yb $L_{\rm III}$ edge to a sum of two Lu $L_{\rm III}$ edges suitably shifted to represent the divalent and trivalent components of the Yb edge.[33] We estimate (somewhat arbitrarily) that the absolute error in this procedure is several percent. Figure 7 shows the absorption data and fits for YbMgCu$_4$ and YbAuCu$_4$ at 300 K. All data are well fit by this procedure except for that of YbCdCu$_4$, which had an additional component $\sim$10 eV above the main edge. This component could be due to multiple scattering effects, and in any case does not affect the parameters extracted from the fits. We show n_f at several

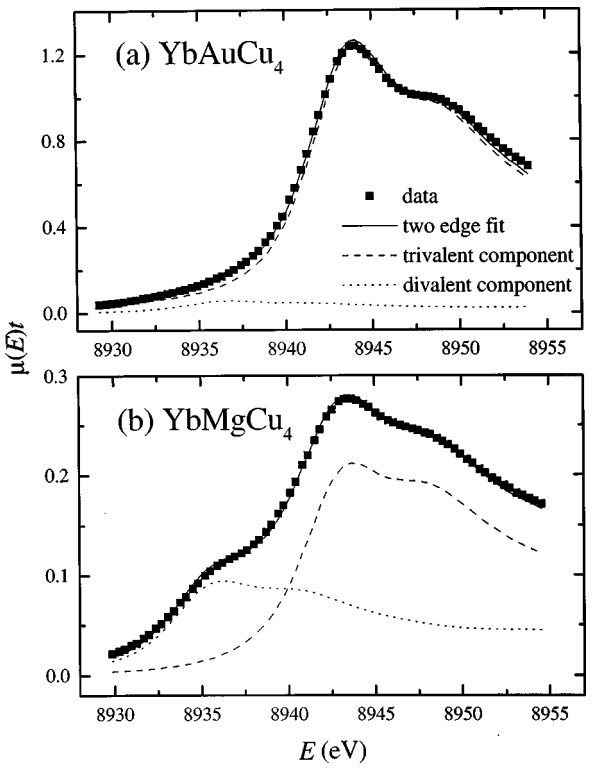

FIG. 7. Example of absorption data and fits to the divalent and trivalent components of the Yb L_{III} edge.

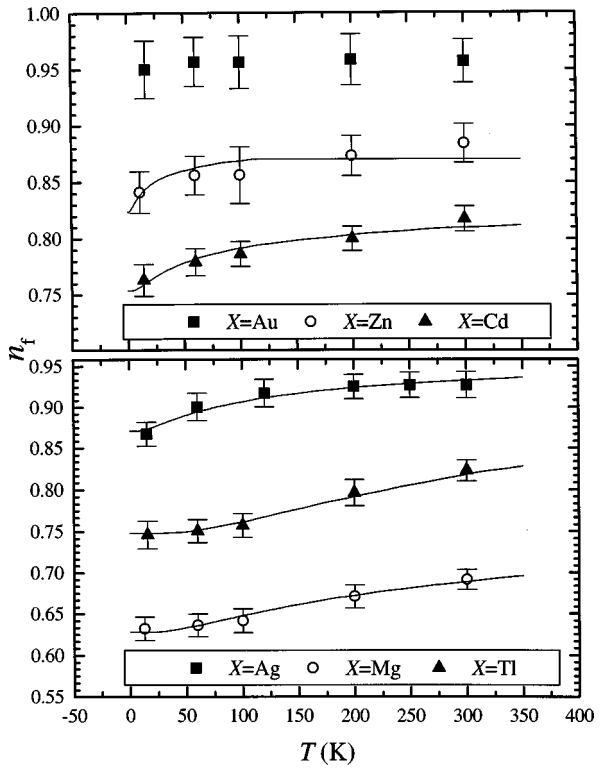

FIG. 8. The number of f electrons per Yb ion n_f as a function of temperature for YbXCu$_4$ (X=Au, Zn, Ag, Cd, Mg, and Tl). Lines are fits to the single impurity model within the NCA approximation (see text).

temperatures ranging from 20–300 K for each of the YbXCu$_4$ compounds in Fig. 8.

Although an exact solution to the single impurity Anderson model for $n_f \neq 1$ does not exist, calculations for $J=5/2$ cerium have been made by Bickers, Cox, and Wilkins within the noncrossing approximation (NCA) for $n_f \neq 1$.[25] The NCA has the advantage that $n_f(T)$ can be input as a parameter to the model together with the Kondo temperature, and other physical quantities can be determined uniquely. The relationship of $n_f(T)$ and T_0 to the strength of f-electron/conduction-electron hybridization $\Gamma=\pi N(0)V^2$, the f-level energy ε_f, and the conduction electron bandwidth D derives from the temperature dependence of n_f:

$$n_f(T)=n_f(\infty)-[\Delta n_f(T)/\Delta n_f(0)]\Delta n_f(0), \tag{4}$$

where

$$\Delta n_f(0)=[1+(\nu\Gamma)/(\pi T_{\mathrm{NCA}})]^{-1}, \tag{5}$$

ν is the spin degeneracy, T_{NCA} is the characteristic temperature in the NCA (note that $T_0 \approx 1.43 T_{\mathrm{NCA}}$) and $\Delta n_f(T)/\Delta n_f(0)$ is a very slowly varying function of $n_f(0)$, given in Ref. 25 for $J=5/2$ and shown to be at least approximately a universal function of J and $n_f(0)$.[25] Therefore, if one has independent measures of $n_f(T)$ and T_0, one can determine Γ. The position of the f-level relates to Γ simply as[32]

$$\varepsilon_f=\frac{\Gamma}{\pi[1-n_f(\infty)]}. \tag{6}$$

Finally, if one has T_{NCA}, Γ, and ε_f, one can calculate the conduction bandwidth D from[32]

$$D=\{T_{\mathrm{NCA}} g^{-1/8} e^{1/(8g)}\}/\{1+D/(T_{\mathrm{NCA}}+\Delta)\}^{3/4}, \tag{7}$$

where $g=\Gamma/(\pi\varepsilon_f)=1-n_f(\infty)$ and Δ is a spin-orbit splitting. Shown in Fig. 8 is a fit using Eq. (4). Assuming T_0's from Table III and extracting $n_f(\infty)$ from the fits in Fig. 8, the resulting values for Γ, ε_f, and D, calculated with Eqs. (4)–(7), are shown in Table IV.

VIII. DISCUSSION

A. Sources of deviation from single-impurity model

There are two general approaches to addressing the fact that single-impurity models do not quantitatively and universally explain all of the phenomena observed in our data for the YbXCu$_4$ compounds. One is to recognize that a model which considers only a single f-ion impurity in a conduction

TABLE IV. Parameters extracted from fits to $n_f(T)$ data [$n_f(\infty)$ and Γ] and the resulting calculated values of ε_f and D. Values of T_0 (based on χ_{fit}) were chosen from Table III and held fixed. The calculation of D does not include crystal-field splitting (for the calculations, recall $T_0 \approx 1.43 T_{\mathrm{NCA}}$).

X	T_0 (K)	$n_f(\infty)$	Γ (K)	ε_f (eV)	D (eV)
Zn	31	0.87(3)	176(5)	0.037(9)	0.004(3)
Cd	101	0.81(3)	444(8)	0.065(10)	0.010(3)
Ag	181	0.95(3)	583(6)	0.3(2)	0.06(5)
Mg	526	0.76(3)	958(9)	0.11(1)	0.05(1)
Tl	900	0.98(3)	706(10)	1(1)	3(3)

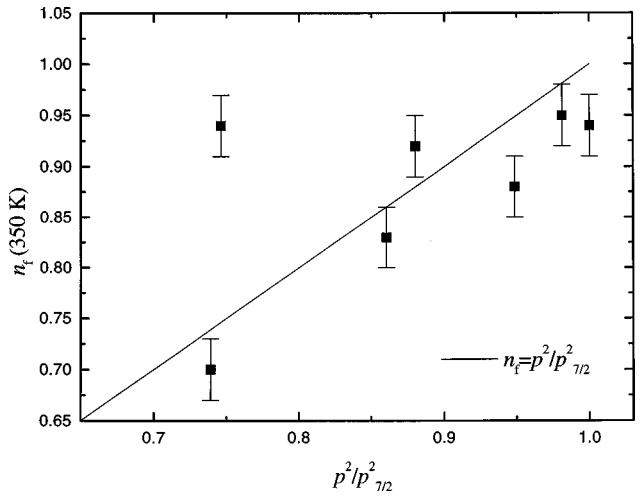

FIG. 9. n_f as a function of the fraction of the full moment $p^2/p^2_{7/2}$ at 350 K (each data point represents a particular YbXCu$_4$). Because the fractional moment is still increasing for the materials with moderately high T_0's, we used the highest temperature data for fits to $1/\chi(T)$ and extrapolated the data for n_f (Fig. 8) to 350 K. To be more accurate, this comparison should be made at temperatures several times T_0 for each material.

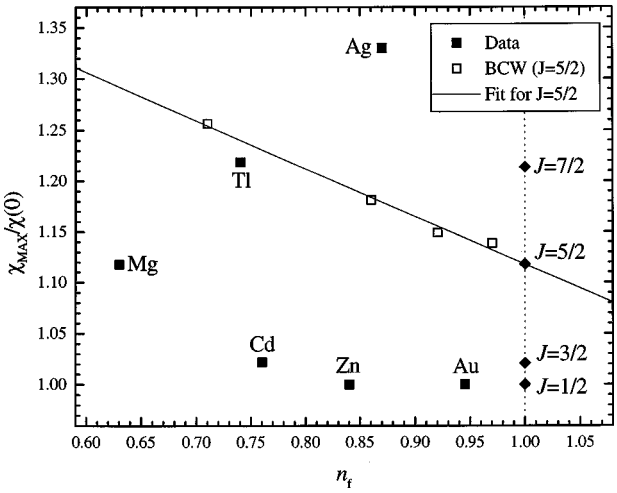

FIG. 10. $\chi_{\max}/\chi(0)$ vs $n_f(T=0)$. Data from BCW (Ref. 25) are normalized to the Bethe ansatz result (Ref. 24) at $n_f=1$.

sea cannot possibly explain the detailed properties of a periodic lattice of f moments. We will discuss those aspects of our data that clearly require periodicity below; however, it is perhaps more constructive to first consider those effects which might modify the predictions of a single-impurity theory without explicitly requiring periodicity.

Because the most quantitative comparisons can be made between our measured $n_f(T)$ and model calculations, we should first convince ourselves that these values are meaningful. As shown in Table I, $1-n_f(T=300\,\mathrm{K})$, as determined from our L_{III} absorption-edge data discussed in Sec. VII, is in qualitative agreement with the difference in lattice volume between YbXCu$_4$ and LuXCu$_4$, a separate measure of the departure of Yb from trivalence at room temperature. As a more quantitative check that n_f is accurately measured by L_{III} absorption, we determined the average magnetic moment p of each Yb ion as a fraction of the moment for a $J=7/2$ lanthanide $p_{7/2}$, assuming a Curie-Weiss law at 350 K, from the magnetic susceptibility data in Fig. 3. We use the highest temperature data available so that we are as close as possible to the temperature region where Curie-Weiss behavior should dominate. Because the divalent state of Yb is not magnetic, and to the extent that susceptibility is an instantaneous probe of the magnetic state, $p^2/p^2_{7/2}$ should equal n_f. In Fig. 9 we have plotted n_f [extrapolated to 350 K using Eq. (4)] as a function of the square of the fractional moment for these materials and found that they agree quite well within an estimated absolute error of 3%, with the exception of Ag, which differs by ~15%. Together the lattice constant and magnetic susceptibility data are strong evidence that the L_{III} data are describing the bulk value of n_f.

Next, we examine the extent to which the other parameters extracted from the fits to $n_f(T)$ using the NCA are physically realistic. The calculated hybridization Γ (Table IV) is within the accepted range of energies, that is, of the order of T_0. The f-level energy ε_f is generally taken to be around 1 eV, but 0.1 eV (as the L_{III} fits suggest) is not out of the question. The most troubling result is the value of the conduction electron bandwidth D. This is usually taken to be around 3 eV. At first glance, the only material for which the fit might be consistent with such a value is YbTlCu$_4$ (Table IV). All of the other YbXCu$_4$ yield values of $D \approx 0.01-0.1$ eV, which is extraordinarily narrow and probably unphysical, raising doubts about the validity of the NCA and the single-impurity model in explaining the observed data. We note, however, that the value of D depends sensitively on the value of $n_f(\infty)$ which is a free parameter of our fit; reasonable values of D correspond to $n_f(\infty)\approx 1$. For YbAgCu$_4$ only small changes in $n_f(\infty)$ are required to obtain physical values of D.

Turning to the magnetic susceptibility data, there are several questions that need to be addressed. Can the observed departures of n_f from the Kondo limit explain the nonuniversal behavior of $\chi_{\max}/\chi(0)$ that we observe? Calculations within the noncrossing approximation for $J=5/2$ indicate that decreasing $n_f(T=0)$ causes $\chi_{\max}/\chi(0)$ to increase,[25] so compound-to-compound variation in $n_f(T=0)$ could explain the absence of universality in our data. In order to examine whether the variation of $\chi_{\max}/\chi(0)$ among the YbXCu$_4$ compounds is due *solely* to variations in $n_f(T=0)$, Fig. 10 shows $\chi_{\max}/\chi(0)$ for each YbXCu$_4$ versus $n_f(T=0)$. To the extent that the data points do not lie on a line parallel to the $J=5/2$ NCA calculation (with the offset determined from the $n_f=1$ Bethe ansatz values), relaxing the constraint that $n_f=1$ does not by itself explain the compound-to-compound variations in the shape of $\chi(T)$.

The best fits to our susceptibility data (Fig. 3) were obtained by using curves for various J from the calculations by Rajan.[24] In these fits, we found that with the exception of YbAgCu$_4$, the J that produced the best fit increased as T_0 increased. Crystal field splitting, which becomes increasingly relevant as T_0 becomes small, could in principle explain the variation in effective J with T_0 and might also explain some of the observed deviation in the Wilson ratio from the value (8/7) expected for a $J=7/2$ Kondo impurity. YbAuCu$_4$ is known to have significant, well-resolved crystal-field splitting, while no such splitting has been observed in YbAgCu$_4$.[5] Realistically, we should make some estimate of

(or better, actually measure) the scale of crystal-field splitting for each of the YbXCu$_4$ (100 K is a zeroth order estimate) and then fit the data with reduced J below this temperature and full J at high temperature. In fact such an analysis has been performed for YbAgCu$_4$.[34] However, because our purpose has been to give a qualitative flavor for the data, we have intentionally avoided this added complexity. Furthermore, large changes in J would greatly affect T_0 as determined from $\chi(0)$, and therefore the qualitative agreement between T_0 from $\chi(0)$ and $\chi_{\rm fit}$ would be destroyed. We therefore feel that crystal fields alone cannot explain fully the variation observed in our data.

The final possibility we raise for explaining the compound-to-compound variations in magnetic susceptibility is that there is a distribution of Kondo temperatures for those YbXCu$_4$ whose susceptibility deviates significantly from the $J=7/2$ Bethe ansatz prediction. This approach has been successfully employed in the analysis of susceptibility and NMR data for UPdCu$_4$.[35] Such a model could be applicable here if the distributions of T_0 were sufficiently narrow as to leave the system in a Fermi-liquid regime, as these materials appear to be. Within this limit, a Kondo-disorder model would allow for a decrease in $\chi_{\rm max}/\chi(0)$ while maintaining the agreement among $\chi(0)$, $T_0(\chi_{\rm fit})$ and the derived Wilson ratios, because these are all mainly sensitive to $\langle T_0 \rangle$, the average Kondo temperature. One possible mechanism for a distribution of Kondo temperatures may be structural disorder. Even though the crystal symmetry is the same for each of the YbXCu$_4$ compounds, it is possible that local structural disorder or distortions are present. The absence of significant coherence-induced decreases in resistivity for some X (see Sec. VI) adds some credence to this argument. In the nominal YbXCu$_4$ crystal structure the Yb-Cu and X-Cu bond distances are identical; however, large variations ($\sim$0.2 Å) exist in the radii of the various X ions and their difference in size from that of Yb. In addition to their global effect on lattice constant, discussed in Sec. III, these ionic size differences are likely to affect the local structure of each YbXCu$_4$. Although we see no direct evidence for this in our diffraction data, X/Cu site disorder is also a possibility, especially for X's such as Zn that have radii comparable to that of Cu. Experiments that probe the local structure and disorder of these materials are currently underway to clarify these issues.

Finally, one must recall that coherence effects associated with the periodic lattice of *f*-moments have to play a role in understanding these materials. The downturn in resistivity for $T<T_0$ observed for many of the YbXCu$_4$ is beyond the scope of any single-impurity model. Although only pressure-dependent resistivity data can rule out crystal-field depopulation as a mechanism for the observed temperature dependence, it is certainly the case that such a mechanism cannot explain the properties of YbAgCu$_4$. The unphysically small bandwidths that are extracted from the NCA fits to the $L_{\rm III}$ data also point to the not-unexpected inadequacy of a single-impurity model in describing periodic Bloch states. Fortunately, progress in treating periodic lattices of *f*-moments theoretically is being made.[36]

B. Chemical trends

Because one does not have a rigorous theory in which to understand self-consistently all of the data for the YbXCu$_4$ compounds, it is constructive to discuss the trends that can be observed. In the simplest terms, varying X in YbXCu$_4$ has two effects: a volume effect associated with ionic size and an electronic effect associated with electron count. Monachesi and Continenza have examined these effects rigorously in the cases of YbAgCu$_4$, YbAuCu$_4$, and YbPdCu$_4$.[37] Although an equally complete treatment of YbMgCu$_4$, YbZnCu$_4$, YbCdCu$_4$, and YbTlCu$_4$ would be valuable, here we limit our discussion to qualitative observations. Because divalent Yb is larger than trivalent Yb, larger X ions push Yb towards trivalence. Ions with more electrons, because of hybridization between Yb and X, favor ''electron-rich'' divalent Yb. In actual materials, of course, one has to consider not only which mechanism dominates but also their coupled interaction (e.g., the extent of hybridization depends on both the density of states at the Fermi energy and the volume of the lattice). Even in isoelectronic materials, e.g., YbAg$_{1-x}$Cu$_x$Cu$_4$ (Refs. 38 and 39) and YbAg$_{1-x}$Au$_x$Cu$_4$,[40] the situation is not always simple: in the former case, a volumetric description has been quite successful, while in the latter, such a description is inadequate.

In our discussion of YbXCu$_4$, one should also recall the recent work on the fcc phase of YbCu$_5$, stabilized by high-pressure synthesis techniques.[22,39,41] Cubic YbCu$_5$, in fact, has the largest linear coefficient of specific heat ($\gamma = 600\,{\rm mJ/mol\,K^2}$) of any of the Yb$XCu_4$ compounds yet reported. Although an analysis as comprehensive as that presented in this study has not yet been completed, the reported experimental data reveal agreement with predictions of the $J=7/2$ Bethe ansatz that rival that of YbAgCu$_4$.

As one moves with X in the periodic table from the lower left to the upper right in the late transition metals, one observes increasingly mixed valence. For $X=$ Au and Pd, ordered magnetism is observed.[4,11] For $X=$ Cu, Ag, Zn, and Cd, nearly trivalent behavior is observed with $T_0 \sim 100\,{\rm K}$, and no magnetic order is observed above 300 mK. Finally, for $X=$ Tl and In (at least in its low temperature state, $T<40\,{\rm K}$) large T_0's ($\sim$500–1000 K) are observed, and YbAlCu$_4$ (Refs. 42 and 43) and YbGaCu$_4$ (Refs. 42 and 44) are, in fact, hexagonal and nonmagnetic. Although one might naively put $X=$ Mg ''on top of Zn'' because Mg is a full shell element, it appears to fit best in this last group. This trend suggests that increasing electron count rather than ionic size variation has the greater impact on Yb valence in the YbXCu$_4$ materials (recall Table I). In this context, it is worth recalling that the first-order valence transition in YbInCu$_4$ appears to be more amenable to an ''electronic'' description than a volumetric one.[14,28]

The more difficult question to answer is how YbAgCu$_4$, YbCdCu$_4$, and YbZnCu$_4$ can be so similar and yet so different, especially as compared to cubic YbCu$_5$. Each X is bigger than Cu, so it is perhaps not surprising that T_0 is increased for each as compared to $X=$ Cu. The variation in J inferred from our susceptibility data may point to variations in hybridization strength like that observed in YbAgCu$_4$ and YbAuCu$_4$,[37] although the T_0's and Γ's deduced from $n_f(T)$ data are comparable. To address this issue, inelastic neutron scattering measurements are underway to study the relative strength of quasielastic and inelastic scattering for YbCdCu$_4$ and YbZnCu$_4$. Finally, given the similarity in size between Zn and Cu, Zn/Cu site disorder may be particularly impor-

tant in this case. Although the lack of clear trends among these materials is somewhat unsettling, it does reveal the complexity and richness of the competition among the mechanisms which determine the physical properties of the YbXCu$_4$ compounds and leaves much room for future study. In fact, YbAgCu$_4$, the most-heavily studied and seemingly understood of the YbXCu$_4$ compounds, may be the most anomalous of the group: each of its physical properties (from lattice constant to magnetic susceptibility and transport) deviates strongly from the behavior observed in the other materials.

IX. CONCLUSION

In summary, we have performed an experimental survey of a wide class of face-centered-cubic YbXCu$_4$ compounds. In particular, comprehensive data for four new members of this family (YbCdCu$_4$, YbMgCu$_4$, YbTlCu$_4$, and YbZnCu$_4$) have been reported. Although the single-impurity model qualitatively accounts for much of the data, universal behavior cannot be inferred by only accounting for variations in the Kondo temperature. Rather, the varied impact of crystal-field splitting, variations in effective valence, hybridization, and, perhaps, disorder conspire to create a situation in which large compound-to-compound variations in physical properties are observed. Although our understanding of these effects is incomplete, the addition of new members to this family of compounds has more clearly defined what we do not understand.

ACKNOWLEDGMENTS

The NHMFL is supported by the NSF and the state of Florida through Cooperative Agreement No. DMR-9527035. Work at LANL is performed under the auspices of the U.S. Department of Energy. Work at Florida State and Irvine was also supported by the NSF through Grants No. DMR-9501529 and No. DMR-9501528, respectively.

*Present address: Los Alamos National Laboratory, Los Alamos, NM 87545.

†Present address: 2235 Ashley Crossing, Apt. 8K, Charleston, SC 29414.

[1] Z. Fisk and M. B. Maple, J. Alloys Compd. **183**, 303 (1992).

[2] E. Bauer, Adv. Phys. **40**, 417 (1991).

[3] For a review, see A. C. Hewson, *The Kondo Problem to Heavy Fermions* (Cambridge University Press, Cambridge, England, 1993).

[4] C. Rossel, K. N. Yang, M. B. Maple, Z. Fisk, E. Zirngiebl, and J. D. Thompson, Phys. Rev. B **35**, 1914 (1987).

[5] A. Severing, A. P. Murani, J. D. Thompson, Z. Fisk, and C.-K. Loong, Phys. Rev. B **41**, 1739 (1990).

[6] P. Schlottmann, J. Appl. Phys. **73**, 5412 (1993).

[7] E. Bauer, R. Hauser, E. Gratz, K. Payer, G. Oomi, and T. Kagayama, Phys. Rev. B **48**, 15 873 (1993).

[8] T. Graf, R. Movshovich, J. D. Thompson, Z. Fisk, and P. C. Canfield, Phys. Rev. B **52**, 3099 (1995).

[9] T. Graf, J. M. Lawrence, M. F. Hundley, J. D. Thompson, A. Lacerda, E. Haanappel, M. S. Torikachvili, Z. Fisk, and P. C. Canfield, Phys. Rev. B **51**, 15 053 (1995).

[10] E. Bauer, E. Gratz, R. Hauser, Le Tuan, A. Galatanu, A. Kottar, H. Michor, W. Perthold, G. Hilscher, T. Kagayama, G. Oomi, N. Ichimiya, and S. Endo, Phys. Rev. B **50**, 9300 (1994).

[11] E. Bauer, P. Fischer, F. Marabelli, M. Ellerby, K. A. McEwen, B. Roessli, and M. T. Fernandes-Dias, Physica B **234-236**, 676 (1997).

[12] J. M. Lawrence, G. H. Kwei, J. L. Sarrao, Z. Fisk, D. Mandrus, and J. D. Thompson, Phys. Rev. B **54**, 6011 (1996).

[13] J. L. Sarrao, C. D. Immer, C. L. Benton, Z. Fisk, J. M. Lawrence, D. Mandrus, and J. D. Thompson, Phys. Rev. B **54**, 12 207 (1996).

[14] A. L. Cornelius, J. M. Lawrence, J. L. Sarrao, Z. Fisk, M. F. Hundley, G. H. Kwei, J. D. Thompson, C. H. Booth, and F. Bridges, Phys. Rev. B **56**, 7993 (1997).

[15] C. D. Immer, J. L. Sarrao, Z. Fisk, A. Lacerda, C. Mielke, and J. D. Thompson, Phys. Rev. B **56**, 71 (1997).

[16] J. M. Lawrence, S. M. Shapiro, J. L. Sarrao, and Z. Fisk, Phys. Rev. B **55**, 14 467 (1997).

[17] B. Kindler, D. Finsterbusch, R. Graf, F. Ritter, W. Assmus, and B. Luthi, Phys. Rev. B **50**, 704 (1994).

[18] J. M. de Teresa, Z. Arnold, A. del Moral, M. R. Ibarra, J. Kamard, D. T. Adroja, and B. Rainford, Solid State Commun. **99**, 911 (1996).

[19] I. Felner and I. Nowik, Phys. Rev. B **33**, 617 (1986); I. Felner *et al.*, *ibid.* **35**, 6956 (1987); I. Nowik *et al.*, *ibid.* **37**, 5633 (1988).

[20] K. Hiraoka, K. Kojima, T. Hihara, and T. Shinohara, J. Magn. Magn. Mater. **140-144**, 1243 (1995).

[21] K. Kojima, Y. Nakai, T. Suzuki, H. Asano, F. Izumi, T. Fujita, and T. Hihara, J. Phys. Soc. Jpn. **59**, 792 (1990).

[22] J. He, N. Tsujii, M. Nakanishi, K. Yoshimura, and K. Kosuge, J. Alloys Compd. **240**, 261 (1996).

[23] A. Iandelli and A. Palenzona, J. Less-Common Met. **25**, 333 (1971).

[24] V. T. Rajan, Phys. Rev. Lett. **51**, 308 (1983).

[25] N. E. Bickers, D. L. Cox, and J. W. Wilkins, Phys. Rev. B **36**, 2036 (1987).

[26] A. C. Hewson and J. W. Rasul, J. Phys. C **16**, 6799 (1983).

[27] B. Bucher, Z. Schlesinger, D. Mandrus, Z. Fisk, J. L. Sarrao, J. F. DiTusa, C. Oglesby, G. Aeppli, and E. Bucher, Phys. Rev. B **53**, 2948 (1996); J. M. Lawrence, T. Graf, M. F. Hundley, D. Mandrus, J. D. Thompson, A. Lacerda, M. S. Torikachvili, J. L. Sarrao, and Z. Fisk, *ibid.* **53**, 12 559 (1996).

[28] E. Figueroa, J. M. Lawrence, J. L. Sarrao, Z. Fisk, M. F. Hundley, and J. D. Thompson, Solid State Commun. **106**, 347 (1998).

[29] J. Diehl, S. Klimm, H. Davideit, E. Baur, S. Horn, U. Klinger, C. Geibel, F. Steglich, E. Bauer, and H. Kirchmayr, in *Proceedings of Physical Phenomena at High Magnetic Fields II*, edited by Z. Fisk, L. P. Gor'kov, D. Meltzer, and J. R. Schrieffer (World Scientific, Singapore, 1995), p. 185.

[30] A. Fert and P. M. Levy, Phys. Rev. B **36**, 1907 (1987).

[31] E. Cattaneo, Z. Phys. B **64**, 317 (1986).

[32] D. L. Cox, Ph.D. dissertation, The Ohio State University, 1985.

[33] J. M. Lawrence, G. H. Kwei, P. C. Canfield, J. G. DeWitt, and A. C. Lawson, Phys. Rev. B **49**, 1627 (1994).

[34] G. Polatsek and P. Bonville, Z. Phys. B **88**, 189 (1992).

[35] O. O. Bernal, D. E. MacLaughlin, H. G. Lukefahr, and B. Andraka, Phys. Rev. Lett. **75**, 2023 (1995).

[36] A. N. Tahvildar-Zadeh, M. Jarrell, and J. K. Freericks, Phys. Rev.

B **55**, 3332 (1997) and references therein.
[37] P. Monachesi and A. Continenza, Phys. Rev. B **54**, 13 558 (1996).
[38] N. Tsujii, J. He, K. Yoshimura, K. Kosuge, H. Michor, K. Kreiner, and G. Hilscher, Phys. Rev. B **55**, 1032 (1997).
[39] K. Yoshimura, N. Tsujii, J. He, M. Kato, K. Kosuge, H. Michor, K. Kreiner, G. Hilscher, and T. Goto, J. Alloys Compd. **262**, 118 (1997).
[40] A. Indinger, E. Bauer, E. Gratz, R. Hauser, G. Hilscher, and T. Holubar, Physica B **206**, 349 (1995).
[41] N. Tsujii, J. He, F. Amita, K. Yoshimura, K. Kosuge, H. Michor, G. Hilscher, and T. Goto, Phys. Rev. B **56**, 8103 (1997).
[42] D. T. Adroja, S. K. Malik, B. D. Padalia, and R. Vijayaraghavan, J. Phys. C **20**, L307 (1987).
[43] E. Bauer, R. Hauser, L. Keller, P. Fischer, O. Trovarelli, J. G. Sereni, J. J. Rieger, and G. R. Stewart, Phys. Rev. B **56**, 711 (1997).
[44] E. Bauer, Le Tuan, R. Hauser, E. Gratz, T. Holubar, G. Hilscher, H. Michor, W. Perthold, C. Godart, E. Alleno, and K. Hiebl, Phys. Rev. B **52**, 4327 (1995).